Inorganic Chemistry
Article

Inorg. Chem. **2010**, *49*, 1905–1912 **1905**
DOI: 10.1021/ic9023713

Syntheses, Structures, and Magnetic Properties of Heterobimetallic Clusters with Tricyanometalate and π-Conjugated Ligands Containing 1,3-Dithiol-2-ylidene

Yan-Hong Peng, Yi-Fei Meng, Liang Hu, Quan-Xiu Li, Yi-Zhi Li, Jing-Lin Zuo,* and Xiao-Zeng You

State Key Laboratory of Coordination Chemistry, School of Chemistry and Chemical Engineering, Nanjing National Laboratory of Microstructures, Nanjing University, Nanjing 210093, People's Republic of China

Received November 30, 2009

Two new π-conjugated 1,3-dithiol-2-ylidene-containing ligands, 4,5-[1′,4′]dithiino[2′,3′-*b*]quinoxaline-2-bis(2-pyridyl)methylene-1,3-dithiole (L_1) and 4,5-bis(methylthio)-2-bis(2-pyridyl)methylene-1,3-dithiole (L_2), have been synthesized and characterized. Using L_1, L_2, or dimethyl 2-[di(pyridin-2-yl)methylene]-1,3-dithiole-4,5-dicarboxylate (L_3) as the auxiliary ligand and $[(Tp)Fe(CN)_3]^-$ or $[(i\text{-}BuTp)Fe(CN)_3]^-$ [Tp = tris(pyrazolyl)borate; *i*-BuTp = 2-methylpropyltris(pyrazolyl)borate] as the building block, two rectangular-square Fe_2Ni_2 clusters $[(Tp)Fe(CN)_3Ni(L_1)_2]_2\cdot 2ClO_4\cdot 6H_2O$ (**1**) and $[(i\text{-}BuTp)Fe(CN)_3Ni(L_3)_2]_2\cdot 2ClO_4\cdot 6H_2O$ (**2**) and two trinuclear clusters $[(Tp)_2Fe_2(CN)_6Ni(L_2)_2]\cdot 8H_2O$ (**3**) and $[(Tp)_2Fe_2(CN)_6Co(L_3)_2]\cdot 5H_2O$ (**4**) have been prepared in parallel and structurally characterized. Complexes **1** and **2** show similar square structures, and weaker intermolecular $\pi-\pi$-stacking interactions through the pyrazolyl groups of the Tp^- ligands are observed. 2D sheet structures are formed in complexes **3** and **4** through intermolecular $\pi-\pi$-stacking interactions. In **3**, shorter S···S contacts further connect the 2D sheets to 3D supramolecular structures. Magnetic studies show intramolecular ferromagnetic coupling in complexes **1**−**4**. Complexes **1** and **2** show obvious frequency dependencies in the alternating-current magnetic susceptibility data, indicating single-molecule-magnet behavior with effective spin-reversal barriers of 8.7 K for **1** and 13.5 K for **2**, respectively.

Introduction

Single-molecule magnets (SMMs) showing magnetic bistability have received extensive research interest because of their potential applications in high-density magnetic storage, quantum computer, and spintronics.[1] Because the cyano bridge is an efficient propagation for magnetic coupling, cyano-bridged clusters or coordination polymers have attracted great attention, especially for studies on SMMs.[2] Among them, tailored tricyanometalate precursors, for example, $[(Tp)Fe(CN)_3]^-$ [Tp = tris(pyrazolyl)borate], have been widely used recently for new cyanide-bridged compounds with interesting structures and magnetic properties.[3,4] Indeed, some SMMs,[5] single-chain magnets,[6] and 3D frameworks[7] have been reported.

---

*To whom correspondence should be addressed. E-mail: zuojl@nju.edu.cn. Fax: +86-25-83314502.

(1) (a) Structure and Bonding. *Single-Molecule Magnets and Related Phenomena*; Winpenny, R., Ed.; Springer: Berlin, 2006; Vol. *122*. (b) Gómez-Segura, J.; Veciana, J.; Ruiz-Molina, D. *Chem. Commun.* **2007**, 3699. (c) Krusin-Elbaum, L.; Shibauchi, T.; Argyle, B.; Gignac, L.; Weller, D. *Nature* **2001**, *410*, 444. (d) Leuenberger, M. N.; Loss, D. *Nature* **2001**, *410*, 789. (e) Bogani, W.; Wernsdorfer, W. *Nat. Mater.* **2008**, *7*, 179. (f) Shatruk, M.; Chambers, K. E.; Prosvirin, A. V.; Dunbar, K. R. *Inorg. Chem.* **2007**, *46*, 5155.

(2) (a) Ito, A.; Suenaga, M.; Ono, K. *J. Chem. Phys.* **1968**, *48*, 3597. (b) Mallah, T.; Thiebaut, S.; Verdaguer, M.; Veillet, P. *Science* **1993**, *262*, 1554. (c) Entley, W. R.; Girolami, G. S. *Science* **1995**, *268*, 397. (d) Ferlay, S.; Mallaah, T.; Ouahès, R.; Veillet, P.; Verdaguer, M. *Nature* **1995**, *378*, 701. (e) Holden, A. N.; Matthias, B. T.; Anderson, R. M.; Lewis, H. W. *Phys. Rev.* **1956**, *102*, 1463. (f) Goodwin, A. L.; Kennedy, B. J.; Kepert, C. J. *J. Am. Chem. Soc.* **2009**, *131*, 6334. (g) Nihei, M.; Ui, M.; Yokota, M.; Han, L. Q.; Maeda, A.; Kishida, H.; Okamoto, H.; Oshio, H. *Angew. Chem., Int. Ed.* **2005**, *44*, 6484. (h) Wilson, D. C.; Liu, S. M.; Chen, X. N.; Meyers, E. A.; Bao, X. G.; Prosvirin, A. V.; Dunbar, K. R.; Hadad, C. M.; Shore, S. G. *Inorg. Chem.* **2009**, *48*, 5725. (i) Zhang, Y. Z.; Sato, O. *Inorg. Chem.* **2009**, ASAP.(j) Sutter, J. P.; Dhers, S.; Rajamani, R.; Ramasesha, S.; Costes, J. P.; Duhayon, C.; Vendier, L. *Inorg. Chem.* **2009**, *48*, 5820. (k) Beltran, L. M. C.; Long, J. R. *Acc. Chem. Res.* **2005**, *38*, 325 and references cited therein.(l) Berlinguette, C. P.; Dunbar, K. R. *Chem. Commun.* **2005**, 2451. (m) Kaye, S. S.; Choi, H. J.; Long, J. R. *J. Am. Chem. Soc.* **2008**, *130*, 16921. (n) Freedman, D. E.; Jenkins, D. M.; Iavarone, A. T.; Long, J. R. *J. Am. Chem. Soc.* **2008**, *130*, 2884.

(3) (a) Lescouëzec, R.; Vaissermann, J.; Lloret, F.; Julve, M.; Verdaguer, M. *Inorg. Chem.* **2002**, *41*, 5943. (b) Lescouëzec, R.; Toma, L. M.; Vaissermann, J.; Verdaguer, M.; Delgado, F. S.; Ruiz-Pérez, C.; Lloret, F.; Julve, M. *Coord. Chem. Rev.* **2005**, *249*, 2691.

(4) (a) Yang, J. Y.; Shores, M. P.; Sokol, J. J.; Long, J. R. *Inorg. Chem.* **2003**, *42*, 1403. (b) Kim, J.; Han, S.; Pokhodnya, K. I.; Migliori, J. M.; Miller, J. S. *Inorg. Chem.* **2005**, *44*, 6983.

(5) (a) Liu, W.; Wang, C. F.; Li, Y. Z.; Zuo, J. L.; You, X. Z. *Inorg. Chem.* **2006**, *45*, 10058. (b) Wang, S.; Zuo, J. L.; Zhou, H. C.; Choi, H. J.; Ke, Y.; Long, J. R.; You, X. Z. *Angew. Chem., Int. Ed.* **2004**, *43*, 5940. (c) Wang, C. F.; Zuo, J. L.; Bartlett, B. M.; Song, Y.; Long, J. R.; You, X. Z. *J. Am. Chem. Soc.* **2006**, *128*, 7162. (d) Wang, C. F.; Gu, Z. G.; Lu, X. M.; Zuo, J. L.; You, X. Z. *Inorg. Chem.* **2008**, *47*, 7957.

(6) (a) Wang, S.; Zuo, J. L.; Gao, S.; Song, Y.; Zhou, H. C.; Zhang, Y. Z.; You, X. Z. *J. Am. Chem. Soc.* **2004**, *126*, 8900. (b) Li, X. M.; Wang, C. F.; Ji, Y.; Kang, L. C.; Zhou, H. C.; Zuo, J. L.; You, X. Z. *Inorg. Chem.* **2009**, *48*, 9166.

(7) (a) Gu, Z. G.; Xu, Y. F.; Kang, L. C.; Li, Y. Z.; Zuo, J. L.; You, X. Z. *Inorg. Chem.* **2009**, *48*, 5073. (b) Jiang, L.; Feng, X. L.; Lu, T. B.; Gao, S. *Inorg. Chem.* **2006**, *45*, 5018.

Scheme 1

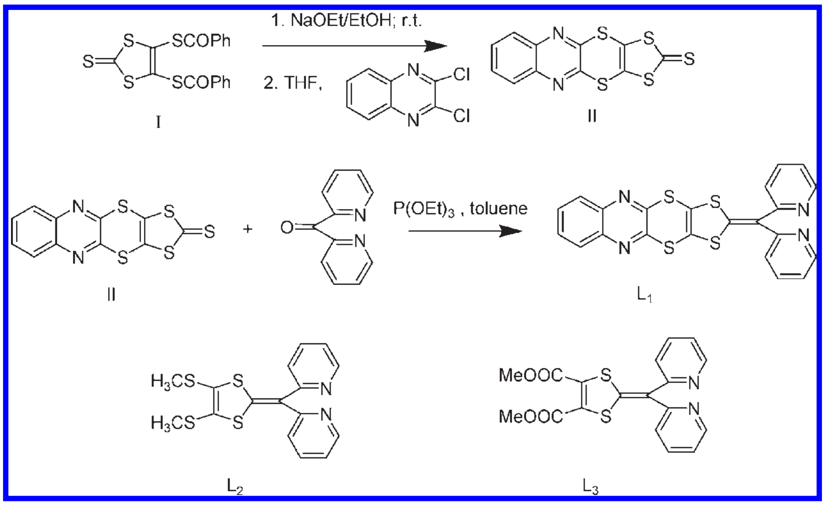

As we know, metal complexes with dithiolene ligands or 1,3-dithiole groups have been studied as molecular conductors and other multifunctional materials.[8] The synthesis of new materials with both metallic conductivity and ferromagnetism has been one of the major challenges in the past few years because of their important applications in molecular spintronics.[9,10] In the literature, some organic ligands containing coupled bis(2-pyridine) groups and 1,2-dithiolenes (or 1,3-dithiol-2-ylidenes) and metal complexes based on them have been prepared.[11−14] In this paper, three π-conjugated ligands containing coupled bis(2-pyridine) groups and 1,3-dithiol-2-ylidenes are introduced in tricyanometalate-based clusters. The reasons for the choice of these π-conjugated sulfur-rich ligands are as follows: (1) investigation of the steric effects of the bulky ligand, which can have pronounced effects on the SMM behavior;[7,15] (2) a conjugated sulfur-rich moiety that may show interchalcogen−atom interactions, which is often observed in molecule-based conductors; (3) attempts to prepare conductive SMMs or molecular magnetic semiconductors.

Herein, two new ligands, 4,5-[1′,4′]dithiino[2′,3′-*b*]quinoxaline-2-bis(2-pyridyl)methylene-1,3-dithiole (L$_1$) and 4,5-bis(methylthio)-2-bis(2-pyridyl)methylene-1,3-dithiole (L$_2$), have been synthesized (Scheme 1). Using L$_1$, L$_2$, or dimethyl 2-[di(pyridin-2-yl)methylene]-1,3-dithiole-4,5-dicarboxylate (L$_3$) as an auxiliary ligand and $[(\mathrm{Tp})\mathrm{Fe(CN)_3}]^-$ or $[(i\text{-}\mathrm{BuTp})\mathrm{Fe(CN)_3}]^-$ [*i*-BuTp = 2-methylpropyltris(pyrazolyl)borate] as a building block, four heterobimetallic complexes, $[(\mathrm{Tp})\mathrm{Fe(CN)_3Ni(L_1)_2}]_2\cdot 2\mathrm{ClO_4}\cdot 6\mathrm{H_2O}$ (**1**), $[(i\text{-}\mathrm{BuTp})\mathrm{Fe(CN)_3Ni(L_3)_2}]_2\cdot 2\mathrm{ClO_4}\cdot 6\mathrm{H_2O}$ (**2**), $[\mathrm{Tp_2Fe_2(CN)_6Ni(L_2)_2}]\cdot 8\mathrm{H_2O}$ (**3**), and $[(\mathrm{Tp})_2\mathrm{Fe_2(CN)_6Co(L_3)_2}]\cdot 5\mathrm{H_2O}$ (**4**), are prepared and structurally characterized. Their magnetic properties are also investigated.

Experimental Section

Materials and Physical Measurements. $(\mathrm{Bu_4N})[(\mathrm{Tp})\mathrm{Fe(CN)_3}]$[3] and $(\mathrm{Bu_4N})[(i\text{-}\mathrm{BuTp})\mathrm{Fe(CN)_3}]$[15a] were prepared by modified literature methods. 4,5-Bis(benzoylthio)-1,3-dithiole-2-thione (I), 4,5-bis(methylthio)-1,3-dithiole-2-thione (III), and L$_3$ were synthesized according to literature methods.[16−18] Other chemicals were reagent-grade and were used as received. Elemental analyses for C, H, N, and S were determined using a Perkin-Elmer 240C analyzer. IR spectra were recorded in the 400−4000 cm^{-1} region by a Vector22 Bruker spectrophotometer with KBr pellets. The magnetic susceptibility measurements of the polycrystalline samples were measured over the temperature range of 1.8−300 K with a Quantum Design MPMS-XL7 SQUID magnetometer under an applied magnetic field from 100 to 2000 Oe. The field dependences of magnetization was measured using a flux magnetometer in an applied field up to 70 kOe generated by a conventional pulsed technique. Data were corrected for the diamagnetic contribution calculated from Pascal constants.[19] The alternating-current (ac) measurements were performed at various frequencies from 1 to

---

(8) (a) Coronado, E.; Day, P. *Chem. Rev.* **2004**, *104*, 5419. (b) Enoki, T.; Miyazaki, A. *Chem. Rev.* **2004**, *104*, 5449. (c) Ouahab, L.; Enoki, T. *Eur. J. Inorg. Chem.* **2004**, 933.

(9) (a) Coronado, E.; Galán-Mascarós, J. R.; Gómez-García, C. J.; Laukhin, V. *Nature* **2000**, *408*, 447. (b) Hiraga, H.; Miyasaka, H.; Nakata, K.; Kajiwara, T.; Takaishi, S.; Oshima, Y.; Nojiri, H.; Yamashita, M. *Inorg. Chem.* **2007**, *46*, 9661. (c) Kosaka, Y.; Yamamoto, H. M.; Nakao, A.; Tamura, M.; Kato, R. *J. Am. Chem. Soc.* **2007**, *129*, 3054. (d) Day, P.; Kurmoo, M. *J. Mater. Chem.* **1997**, *7*, 1291. (e) Motokawa, N.; Miyasaka, H.; Yamashita, M.; Dunbar, K. R. *Angew. Chem., Int. Ed.* **2008**, *47*, 7760.

(10) Gavrilenko, K. S.; Gal, Y. L.; Cador, O.; Golhen, S.; Ouahab, L. *Chem. Commun.* **2007**, 280.

(11) (a) Sako, K.; Misaki, Y.; Fujiwara, M.; Maitani, T.; Tanaka, K.; Tatemitsu, H. *Chem. Lett.* **2002**, 592. (b) Sako, K.; Kusakabe, M.; Tatemitsu, H. *Mol. Cryst. Liq. Cryst.* **1996**, *285*, 101.

(12) (a) Zhu, Q. Y.; Dai, J.; Jia, D. X.; Cao, L. H.; Lin, H. H. *Eur. J. Inorg. Chem.* **2004**, *24*, 4789. (b) Zhu, Q. Y.; Zhang, Y.; Dai, J.; Bian, G. Q.; Jia, D. X.; Zhang, J. S.; Guo, L. *Chem. Lett.* **2003**, *32*, 762. (c) Zhu, Q. Y.; Bian, G. Q.; Dai, J.; Jia, D. X.; Zhang, J. S.; Guo, L. *Inorg. Chim. Acta* **2003**, *351*, 177. (d) Zhu, Q. Y.; Lu, W.; Zhang, Y.; Bian, G. Q.; Gu, J.; Lin, X. M.; Dai, J. *Eur. J. Inorg. Chem.* **2008**, 230.

(13) (a) Baudron, S. A.; Hosseini, M. W. *Inorg. Chem.* **2006**, *45*, 5260. (b) Takahashi, K.; Kawakami, T.; Gu, Z. Z.; Einaga, Y.; Fujishima, A.; Sato, O. *Chem. Commun.* **2003**, 2374.

(14) (a) Liu, W.; Wang, R.; Zhou, X. H.; Zuo, J. L.; You, X. Z. *Organometallics* **2008**, *27*, 126. (b) Liu, W.; Chen, Y.; Wang, R.; Zhou, X. H.; Zuo, J. L.; You, X. Z. *Organometallics* **2008**, *27*, 2990. (c) Chen, Y.; Liu, W.; Jin, J. S.; Liu, B.; Zou, Z. G.; Zuo, J. L.; You, X. Z. *J. Organomet. Chem.* **2009**, *694*, 763.

(15) (a) Wang, C. F.; Liu, W.; Song, Y.; Zhou, X. H.; Zuo, J. L.; You, X. Z. *Eur. J. Inorg. Chem.* **2008**, 717. (b) Li, D. F.; Clérac, R.; Parkin, S.; Wang, G. B.; Yee, G. T.; Holmes, S. M. *Inorg. Chem.* **2006**, *45*, 5251. (c) Li, D. F.; Parkin, S.; Clérac, R.; Holmes, S. M. *Inorg. Chem.* **2006**, *45*, 7569.

(16) (a) Steimecke, G.; Sieler, H. J.; Kirmse, R.; Hoyer, E. *Phosphorus Sulfur* **1979**, *7*, 49. (b) Moses, P. R.; Chambers, J. Q. *J. Am. Chem. Soc.* **1974**, *96*, 945.

(17) Parg, R. P.; Kilburn, J. D.; Petty, M. C.; Pearson, C.; Ryan, T. G. *Synthesis* **1994**, 613.

(18) Chen, Y.; Liu, W.; Liu, B.; Zhou, X. H.; Zou, Z. G.; Zuo, J. L.; You, X. Z. *Inorg. Chim. Acta* **2009**, *362*, 143.

(19) Wertz, J. E.; Bolton, J. R. *Electron Spin Resonance: Elementary Theory and Practical Applications*; Chapman and Hall: New York, 1986.

Table 1. Crystallographic Data for Complexes **1**−**4**

	1·2ClO$_4$·6H$_2$O	**2**·2ClO$_4$·6H$_2$O	**3**·8H$_2$O	**4**·5H$_2$O
formula	$C_{112}H_{80}B_2Cl_2Fe_2N_{34}Ni_2O_{14}S_{16}$	$C_{104}H_{104}B_2Cl_2Fe_2N_{26}Ni_2O_{30}S_8$	$C_{56}H_{62}B_2Fe_2N_{22}NiO_8 S_8$	$C_{60}H_{58}B_2CoFe_2N_{22}O_{13}S_4$
M_r	2960.70	2776.25	1619.79	1615.77
cryst syst	triclinic	triclinic	monoclinic	monoclinic
space group	$P\bar{1}$	$P\bar{1}$	$C2/c$	$P2_1/c$
a (Å)	14.668(2)	14.0971(14)	16.1596(19)	16.1743(17)
b (Å)	14.929(2)	16.2489(17)	28.147(4)	30.125(3)
c (Å)	18.808(3)	17.8026(18)	18.708(2)	22.2805(18)
α(deg)	99.914(2)	66.554(2)	90	90
β (deg)	91.470(3)	80.021(3)	100.344(3)	125.033(5)
γ (deg)	101.981(2)	86.640(2)	90	90
V (Å^3)	3960.7(10)	3684.4(6)	8370.9(18)	8889.3(15)
Z	1	1	4	4
ρ_c (g cm^{-3})	1.241	1.235	1.285	1.207
F(000)	1510	1413	3336	3316
T (K)	291(2)	291(2)	291(2)	291(2)
μ(Mo Kα) (mm $^{-1}$)	0.719	0.665	0.822	0.662
index ranges	$-17 \leq h \leq 18$	$-17 \leq h \leq 16$	$-14 \leq h \leq 19$	$-19 \leq h \leq 19$
	$-18 \leq k \leq 18$	$-20 \leq k \leq 13$	$-34 \leq k \leq 32$	$-36 \leq k \leq 37$
	$-15 \leq l \leq 23$	$-21 \leq l \leq 20$	$-23 \leq l \leq 15$	$-27 \leq l \leq 25$
GOF(F^2)	1.092	0.997	0.965	1.030
R1^a, wR2^b [$I > 2\sigma(I)$]	0.0588, 0.1027	0.0510, 0.0935	0.0706, 0.2062	0.0440, 0.0884
R1^a, wR2^b(all data)	0.0913, 0.1077	0.0809, 0.0997	0.1259, 0.2373	0.0671, 0.0929

^{a} R1 $= \sum||F_o| - |F_c||/\sum|F_o|$. ^{b} wR2 $= [\sum w(F_o^2 - F_c^2)^2/\sum w(F_o^2)]^{1/2}$.

1500 Hz with an ac field amplitude of 5 Oe and no direct-current (dc) field applied.

Caution! *Cyanides are toxic, and perchlorate salts are potentially explosive. Thus, these starting materials should be handled in small quantities and with great caution!*

Synthesis of 1′,3′-Dithiolo[4′,5′:5,6][1,4]dithiino[2,3-*b*]quinoxaline-2-thione (II). Compound II was prepared by modified literature methods.[20] To the suspension of I (16.2 g, 40 mmol) in ethanol was added a solution of Na (1.86 g) in 10 mL of ethanol. The mixture turned red, 50 mL of tetrahydrofuran was added, and then 2,3-dichloroquinoxaline (7.96 g, 40 mmol) was added in one portion. The reaction mixture was stirred at room temperature overnight. A yellow precipitate was obtained after filtration. The products were washed with water and methanol (MeOH), and yellow crystals were obtained after recrystallization from toluene. Yield: 78%. Anal. Calcd for $C_{11}H_4N_2S_5$: C, 40.72; H, 1.24; N, 8.63; S, 49.41. Found: C, 41.0; H, 1.26; N, 8.45; S, 49.29. IR (KBr, cm^{-1}): 1077 (C=S). MS: m/z 324 (M$^+$).

Synthesis of L$_1$. Under a nitrogen atmosphere, the reaction mixture of compound II (0.972 g, 3 mmol) and di-2-pyridyl ketone (0.552 g, 3 mmol) in 3 mL of P(OEt)$_3$ and 20 mL of toluene was refluxed at 110 °C for 10 h and then cooled to room temperature. Orange products were obtained by chromatography on silica with CH$_2$Cl$_2$ as the eluent. Yield: 20%. Anal. Calcd for $C_{22}H_{12}N_4S_4$: C, 57.37; H, 2.62; N, 12.16; S, 27.85. Found: C, 57.58; H, 2.52; N, 12.20; S, 27.7. MS: m/z 461 (M$^+$). IR (KBr, cm^{-1}): 1461, 1635 (C=C). ^{1}H NMR (500 MHz, CDCl$_3$, ppm): δ 8.81 (d, 2H), 8.19 (d, 2H), 8.00 (d, 2H), 7.79 (m, 2H), 7.62 (t, 2H), 7.47 (t, 2H).

Synthesis of L$_2$. L$_2$ was prepared from III in a method similar to that of L$_1$. Light-yellow block crystals were isolated after chromatography and recrystallization. Yield: 40%. Anal. Calcd for $C_{16}H_{14}N_2S_4$: C, 53.00; H, 3.89; N, 7.73; S, 35.37. Found: C, 52.86; H, 3.80; N, 7.84; S, 35.49. MS: m/z 363 (M$^+$). IR (KBr, cm^{-1}): 1463 (−CH$_3$), 1579 (C=C). ^{1}H NMR (500 MHz, CDCl$_3$, ppm): δ 8.79 (d, 2H), 7.72 (t, 2H), 7.20 (t, 2H), 7.13 (d, 2H), 2.45 (m, 3H).

[(Tp)Fe(CN)$_3$Ni(L$_1$)$_2$]$_2$·2ClO$_4$·6H$_2$O (1). A solution of L$_1$ (4.6 mg, 0.01 mmol) in 5 mL of CH$_2$Cl$_2$ was added to a solution of Ni(ClO$_4$)$_2$·6H$_2$O (3.7 mg, 0.01 mmol) in 5 mL of MeOH. The mixture was stirred 10 min, and then a solution of (Bu$_4$N)-[(Tp)Fe(CN)$_3$] (5.9 mg, 0.01 mmol) in 5 mL of MeOH was added. Red rhombic crystals of **1** were obtained after 2 days upon evaporation of the solution. Yield: 70%. Anal. Calcd for $C_{112}H_{80}B_2Cl_2Fe_2N_{34}Ni_2O_{14}S_{16}$: C, 45.44; H, 2.73; N, 16.09; S, 17.33. Found: C, 45.35; H, 2.75; N, 16.01; S, 17.20. IR (KBr, cm^{-1}): 2127 (ν-CN), 2161 (ν_μ-CN).

[(*i*-BuTp)Fe(CN)$_3$Ni(L$_3$)$_2$]$_2$·2ClO$_4$·6H$_2$O (2). A solution of (Bu$_4$N)[(*i*-BuTp)Fe(CN)$_3$] (6.5 mg, 0.01 mmol) in 10 mL of MeOH was added to a solution of Ni(L$_3$)$_2$(ClO$_4$)$_2$ (10 mg, 0.01 mmol) in 10 mL of CH$_2$Cl$_2$. Red crystals of **2** formed after evaporation of the solution. Yield: 80%. Anal. Calcd for $C_{104}H_{104}B_2Cl_2Fe_2N_{26}Ni_2O_{30}S_8$: C, 44.99; H, 3.78; N, 13.12; S, 9.24. Found: C, 44.97; H, 3.85; N, 13.10; S, 9.42. IR (KBr, cm^{-1}): 2033 (ν-CN), 2163 (ν_μ-CN).

[(Tp)$_2$Fe$_2$(CN)$_6$Ni(L$_2$)$_2$]·8H$_2$O (3). A solution of L$_2$ (3.6 mg, 0.01 mmol) in 5 mL of CH$_2$Cl$_2$ was added to a solution of Ni(ClO$_4$)$_2$·6H$_2$O (3.7 mg, 0.01 mmol) in 5 mL of MeOH, followed by the addition of a solution of (Bu$_4$N)[(Tp)Fe(CN)$_3$] (5.9 mg, 0.01 mmol) in 5 mL of MeOH. Red block crystals of **4** were obtained after slow evaporation of the solution. Yield: 50%. Anal. Calcd for $C_{56}H_{62}B_2Fe_2N_{22}NiO_8S_8$: C, 41.52; H, 3.85; N, 19.02; S, 15.84. Found: C, 41.35; H, 3.87; N, 18.99; S, 15.82. IR (KBr, cm^{-1}): 2123 (ν-CN), 2161 (ν_μ-CN).

[(Tp)$_2$Fe$_2$(CN)$_6$Co(L$_3$)$_2$]·5H$_2$O (4). A solution of L$_3$ (3.9 mg, 0.01 mmol) in 5 mL of CH$_2$Cl$_2$ was added to a solution of Co(ClO$_4$)$_2$·6H$_2$O (3.7 mg, 0.01 mmol) in 5 mL of MeOH, and then a solution of (Bu$_4$N)[(Tp)Fe(CN)$_3$] (5.9 mg, 0.01 mmol) in 5 mL of MeOH was added. Red crystals of **3** were obtained after slow evaporation of the solution. Yield: 50%. Anal. Calcd for $C_{60}H_{58}B_2CoFe_2N_{22}O_{13}S_4$: C, 44.60; H, 3.62; N, 19.07; S, 7.94. Found: C, 44.65; H, 3.56; N, 19.15; S, 8.02. IR (KBr, cm^{-1}): 2082 (ν-CN).

X-ray Crystallography. The crystal structures of complexes **1**−**4** were determined on a Siemens (Bruker) SMART CCD diffractometer using monochromated Mo Kα radiation (λ = 0.710 73 Å). Cell parameters were retrieved using *SMART* software and refined using *SAINT*[21] on all observed reflections. Data were collected using a narrow-frame method with scan widths of 0.30° in ω and an exposure time of 10 s frame^{-1}. The highly redundant data sets were reduced using *SAINT* and

---

[20] Varma, K. S.; Edge, S.; Underhill, A. E. *J. Chem. Soc., Perkin Trans. 1* **1990**, 2563.

[21] *SAINT-Plus*, version 6.02; Bruker Analytical X-ray Systems: Madison, WI, **1999**.

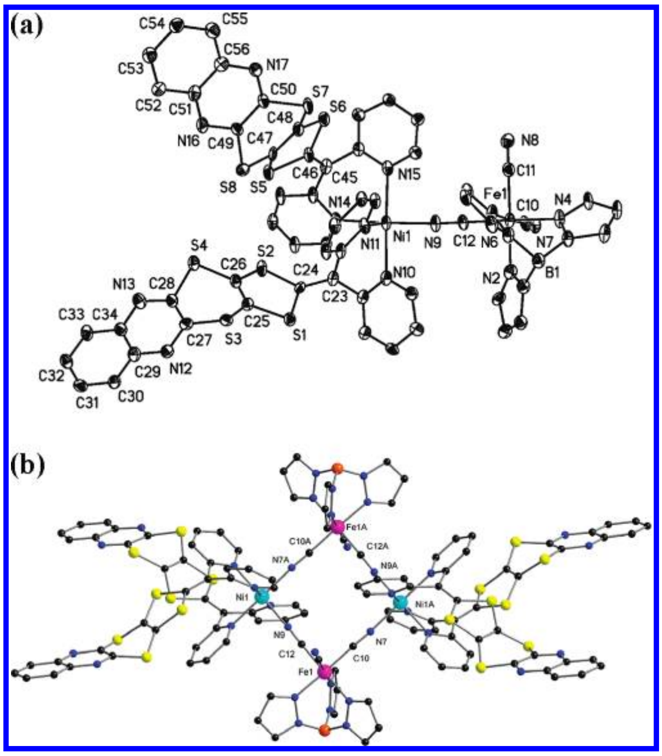

Figure 1. Top: ORTEP view of the asymmetric unit of complex **1** showing the atom numbering. Thermal ellipsoids are drawn at the 50% probability level. Bottom: Structure of the rectangular cluster $[(Tp)Fe(CN)_3Ni(L_1)_2]_2^{2+}$. Hydrogen atoms and solvated molecules are omitted for clarity.

corrected for Lorentz and polarization effects. Absorption corrections were applied using *SADABS*[22] (supplied by Bruker). Structures were solved by direct methods using the program *SHELXL-97*.[23] The positions of the metal atoms and their first coordination spheres were located from direct-method *E* maps; other non-hydrogen atoms were found using alternating difference Fourier syntheses and least-squares refinement cycles and, during the final cycles, were refined anisotropically. Hydrogen atoms were placed in calculated positions and refined as riding atoms with a uniform value of U_{iso}. Information for crystallographic data collection and structure refinement is summarized in Table 1. Selected bond distances and angles are listed in Tables S1−S4 in the Supporting Information, respectively.

Results and Discussion

All ligands were prepared by an unsymmetrical cross-coupling reaction from 1,3-dithiole-2-thione and di-2-pyridyl ketone in $P(OEt)_3$ (Scheme 1). L_3 was prepared in good yield, but L_1 and L_2 were obtained with relatively lower yield. All three ligands are soluble in common organic solvents, such as dichloromethane, chloroform, *N*,*N*-dimethylformamide, and dimethyl sulfoxide. Using L_1−L_3 as the auxiliary ligands and $[(Tp)Fe(CN)_3]^-$ or $[(i\text{-}BuTp)Fe(CN)_3]^-$ as a building block, four heterobimetallic complexes, **1**−**4**, have been prepared. The IR spectra of **1**−**4** exhibit stretching vibrations of C≡N at 2127 and 2161 cm^{-1} for **1**, 2033 and 2163 cm^{-1} for **2**, 2123 and 2161 cm^{-1} for **3**, and 2082 cm^{-1} for **4**, which are comparable to those of other reported similar compounds.[5a,15]

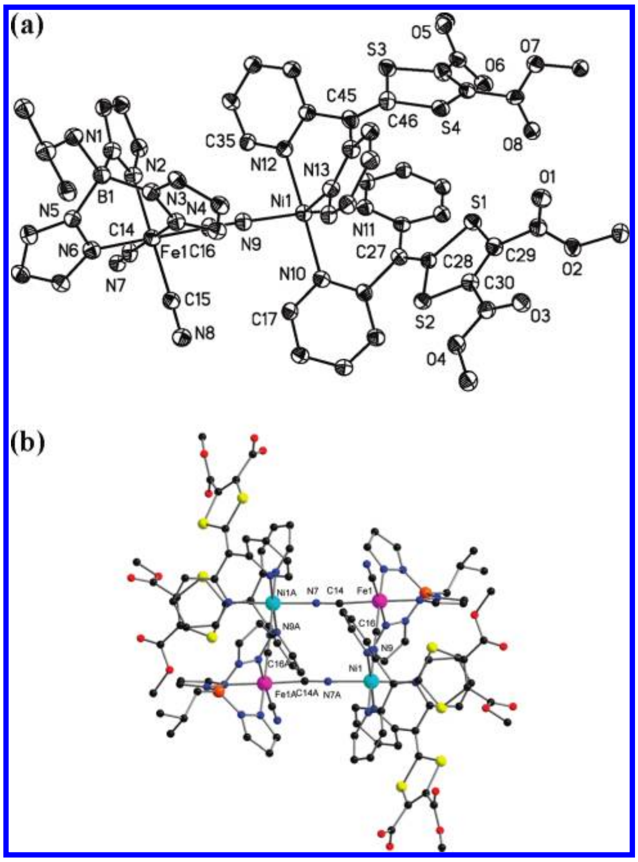

Figure 2. Top: ORTEP view of the asymmetric unit of complex **2** showing the atom numbering. Thermal ellipsoids are drawn at the 50% probability level. Bottom: Structure of the rectangular cluster $[i\text{-}BuTpFe(CN)_3Ni(L_3)_2]_2^{2+}$. Hydrogen atoms and solvated molecules are omitted for clarity.

Crystal Structures. Complexes **1** and **2** have similar rectangular structures. In the square units, Fe^{III} and Ni^{II} ions reside in alternating corners of the rectangle and are bridged by cyanides. Each Ni^{II} ion is linked to two $[TpFe(CN)_3]^-$ or $[i\text{-}BuTpFe(CN)_3]^-$ units at the cis positions; each $[(Tp)Fe(CN)_3]^-$ or $[i\text{-}BuTpFe(CN)_3]^-$ unit uses its two cyanides to connect Ni^{II} ions, leaving the third terminal cyanide group free. The bond lengths and angles in the $[(Tp)Fe(CN)_3]^-$ unit of clusters **1** and **2** are close to those in low-spin cyano-containing Fe^{III} complexes.[5,6,24]

For **1** and **2**, the nickel atoms are six-coordinated as a distorted octahedron of NiN_6 (Figures 1 and 2). The equatorial coordination sites of **1** are occupied by four nitrogen atoms (N10, N11, N14, and N15) from two L_1 auxiliary ligands, and the axial positions of Ni1 are occupied by two cyanide groups (N7A and N9); in **2**, the equatorial coordination sites of Ni1 are occupied by nitrogen atoms (N7A and N9) from two cyanide bridges and nitrogen atoms (N10 and N12) from two L_3 ligands, and the axial positions of Ni1 are occupied by nitrogen atoms (N11 and N13) from L_3.

The Fe−C≡N and Ni−N≡C angles are in the ranges of 176.0(2)−179.2(3)° and 175.5(3)−177.9(2)°, which are

---

[22] Sheldrick, G. M. *SADABS, An empirical absorption correction program*; Bruker Analytical X-ray Systems: Madison, WI, **1996**.

[23] Sheldrick, G. M. *SHELXTL-97*; Universität of Göttingen: Göttingen, Germany, **1997**.

[24] (a) Oshio, H.; Onodera, H.; Tamada, O.; Mizutani, H.; Hikichi, T.; Ito, T. *Chem.*−*Eur. J.* **2000**, *6*, 2523. (b) Oshio, H.; Yamamoto, M.; Ito, T. *Inorg. Chem.* **2002**, *41*, 5817. (c) Kou, H. Z.; Gao, S.; Li, C. H.; Liao, D. Z.; Zhou, B. C.; Wang, R. J.; Li, Y. D. *Inorg. Chem.* **2002**, *41*, 4756.

quite close to linearity. The bis(2-pyridyl) part of L_1 and L_3 forms a "butterfly-like" substructure like that in other bpydt derivatives.[14,18] In **1**, the dihedral angle between plane A (formed by the central C23=C24 bond, S1, and S2 of the 1,3-dithiole ring) and plane B (formed by S1, C25, C26, and S2 of the 1,3-dithiole ring and S3 and S4) is 157.8(4)°. Plane C (C27, C28, N12, N13, C29, C30, C31, C32, C33, and C34) deviates from plane B with a dihedral angle of 140.0(7)°. Planes A−C give a chair configuration. The intramolecular Fe···Ni distances are 5.120(4) and 5.135(4) Å, and the Fe···Fe and Ni···Ni separations are 7.371(7) and 7.129(7) Å, respectively. In **2**, the central C23=C24 bond, the five-membered 1,3-dithiole ring (C24, S1, C25, C27, and S2), S3, and S4 are nearly in one plane. The intramolecular Fe···Ni and Fe···Fe separations through bridging cyanides are 4.978(9) and 8.759(1) Å, respectively.

The pyrazolyl rings (N5, N6, C7, C8, and C9 for **1** and N3, N4, C8, C9, and C10 for **2**) from adjacent clusters are parallel to each other, and the shorter intermolecular pyrazolyl−pyrazolyl separation [3.673(3) Å for **1** and 3.721(3) Å for **2**] indicates the existence of weak $\pi-\pi$-stacking interactions, which results in the 1D chains (Figures S1 and S2 in the Supporting Information). For **1**, the shortest intermolecular Fe···Fe, Fe···Ni, and Ni···Ni separations are 7.935(1), 10.752(2), and 14.668(2) Å, respectively. For **2**, the shortest intermolecular Fe···Fe, Fe···Ni, and Ni···Ni separations are 7.691(7), 12.480(1), and 14.097(1) Å, respectively.

The molecular structures for trinuclear complexes **3** and **4** with their atom numbering scheme are depicted in Figures 3 and 4. Two $[\mathrm{TpFe(CN)_3}]^-$ units bridge the central metallic atoms ($\mathrm{Ni^{II}}$ for **3** and $\mathrm{Co^{II}}$ for **4**) through cyano bridges as monodentate ligands. The bond lengths and angles in the $[\mathrm{(Tp)Fe(CN)_3}]^-$ unit are similar to those observed in other complexes.[3a,5d,25,26]

For **3**, the cyanides bridged to the nickel ions are in a bent fashion with a Ni−N≡C bond angle of 159.6(4)°, which is similar to those of other trinuclear complexes.[27] The Ni1−N(cyano) bond distance is 2.054(5) Å, which is slightly shorter than the Ni1−N(L_2) bond lengths [2.118(4)−2.125(4) Å]. The bis(2-pyridyl) part of L_2 also forms a "butterfly-like" substructure. The central C23=C24 bond, the five-membered 1,3-dithiole ring (C24, S1, C25, C27, and S2), S3, and S4 are nearly in one plane. The intramolecular Fe···Ni and Fe···Fe separations through bridging cyanides are 4.978(9) and 8.759(1) Å, respectively. Because of the steric effect of the auxiliary ligands, a large deviation of the N9−Ni1−N9A angle [92.4(2)°] from linearity is observed.

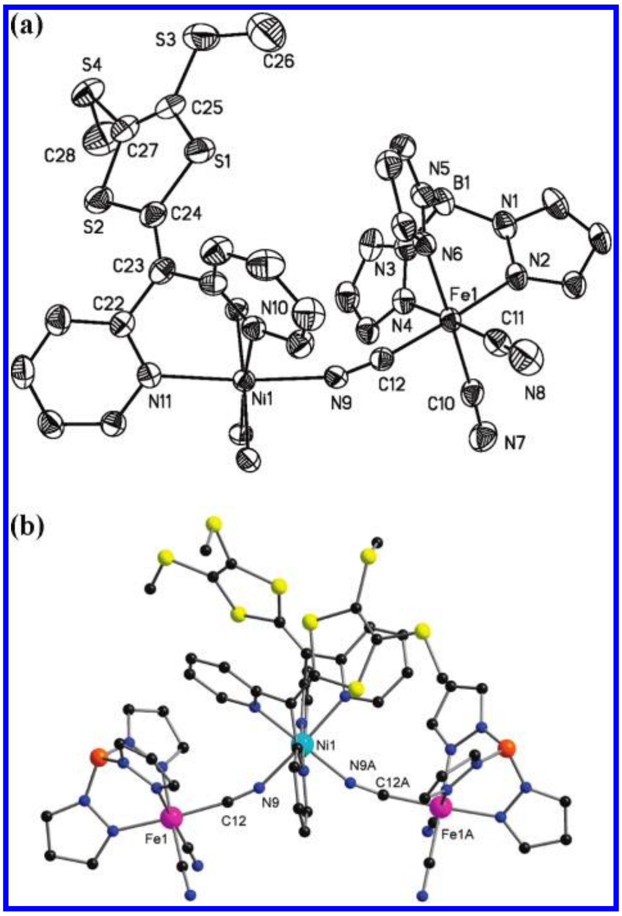

Figure 3. Top: ORTEP view of the asymmetric unit of complex **3** showing the atom numbering. Thermal ellipsoids are drawn at the 30% probability level. Bottom: Structure of the trinuclear cluster $[\mathrm{(Tp)_2Fe_2(CN)_6}$-$\mathrm{Ni(L_2)_2}]$. Hydrogen atoms and solvated molecules are omitted for clarity.

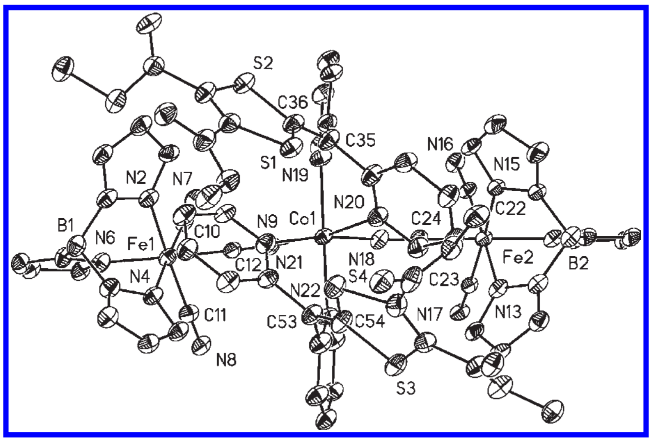

Figure 4. ORTEP view of the asymmetric unit of complex **4** showing the atom numbering. Thermal ellipsoids are drawn at the 50% probability level. Hydrogen atoms and solvated molecules are omitted for clarity.

There are weak intermolecular S···S contacts [3.655(3) Å for S1···S4 and 3.680(3) Å for S2···S3] between the 1,3-dithiolene rings from adjacent clusters, leading to the 1D chain along the *a* axis. These 1D chains are connected through intermolecular $\pi-\pi$-stacking interactions [between the pyrazolyl rings (N5, N6, C7, C8, and C9) of adjacent molecules with a centroid···centroid distance of 3.540(3) Å] to form 2D sheets (Figure S3 in the Supporting Information). Other weak intermolecular $\pi-\pi$-stacking interactions of 3.580(3) Å between the pyrazolyl rings (N1, N2, C1, C2, and C3) from adjacent molecules are also observed. The intermolecular $\pi-\pi$-stacking interactions and shorter S···S contacts give a 3D supramolecular

---

(25) (a) Lescouëzec, R.; Lloret, F.; Julve, M.; Vaissermann, J.; Verdaguer, M.; Llusar, R.; Uriel, S. *Inorg. Chem.* **2001**, *40*, 2065. (b) Lescouëzec, R.; Vaissermann, J.; Ruiz-Pérez, C.; Lloret, F.; Carrasco, R.; Julve, M.; Verdaguer, M.; Dromzee, Y.; Gatteschi, D.; Wernsdorfer, W. *Angew. Chem., Int. Ed.* **2003**, *42*, 1483. (c) Lescouëzec, R.; Lloret, F.; Julve, M.; Vaissermann, J.; Verdaguer, M. *Inorg. Chem.* **2002**, *41*, 818.

(26) Oshio, H.; Tamada, O.; Onodera, H.; Ito, T.; Ikoma, T.; Tero-Kubota, S. *Inorg. Chem.* **1999**, *38*, 5686.

(27) Wang, S.; Zuo, J. L.; Zhou, H. C.; Song, Y.; Gao, S.; You, X. Z. *Eur. J. Inorg. Chem.* **2004**, 3681.

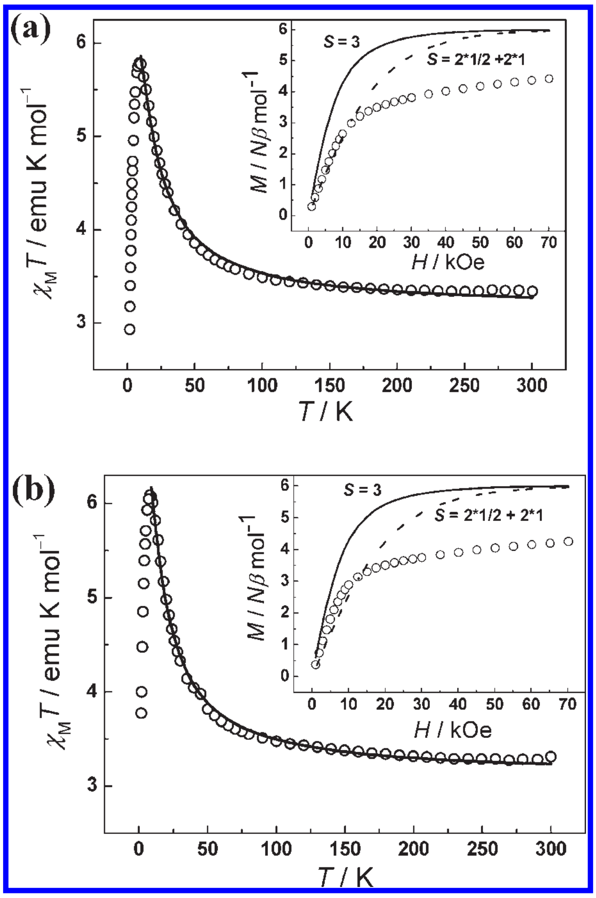

Figure 5. Plots of $\chi_M T$ vs T for **1** (a) and **2** (b) at a field of 2 kOe. Solid lines represent the best fitting of the data. The insets show magnetization versus field up to $H = 70$ kOe at 1.8 K; the lines represent the Brillouin function that corresponds to noninteracting $S = 2S_{\mathrm{Fe}}^{\mathrm{III}} + 2S_{\mathrm{Ni}}^{\mathrm{II}}$ (dotted) and $S = 3$ (solid) with $g = 2.0$.

structure for complex **3** (Figure S5 in the Supporting Information). The shortest intermolecular Fe···Fe, Fe···Ni, and Ni···Ni separations are 7.754(1), 12.137(2), and 14.529(2) Å, respectively.

For complex **4**, the central Co$^{\mathrm{II}}$ ion is six-coordinated in a distorted octahedral coordination environment like those of complexes **1**−**3**. The equatorial coordination sites of Co1 are occupied by four nitrogen atoms (N19, N20, N21, and N22) from two L_3 ligands, and the axial positions of Co1 are occupied by two nitrogen atoms (N18 and N9) from two cyanide bridges. The Fe−N≡C bond angles [174.51(18)° and 172.68(17)°] are quite close to linearity. The Co−N≡C bond angles are 156.92(14)° and 157.83(14)° and deviate from strict linearity. The intramolecular Fe···Ni and Fe···Fe separations through bridging cyanides are 4.977(7) and 8.827(1) Å, respectively.

The π−π-stacking interactions from the pyrazolyl rings [3.493(3) Å] lead to the 1D chainlike structures along the a axis (Figure S6 in the Supporting Information). The 1D chains are further connected through intermolecular π−π-stacking interactions [3.559(3) Å] to form 2D sheets (Figure S7 in the Supporting Information). No intermolecular S···S contact or hydrogen-bonding interaction is found in cluster **4**. The shortest intermolecular Fe···Fe, Fe···Co, and Co···Co separations are 7.746(9), 10.282(1), and 11.490(1) Å, respectively.

Magnetic Properties. Magnetic measurements were performed on polycrystalline samples of complexes **1**−**4**. The temperature dependencies of susceptibility under 2 kOe for **1** and **2** are displayed in Figure 5. At room temperature, the $\chi_M T$ values are 3.34 and 3.35 emu K mol^{-1} for **1** and **2**, respectively, which are somewhat above the spin-only value of 2.75 emu K mol^{-1} ($g = 2.0$) for the $\mathrm{Fe^{III}}_2\mathrm{Ni^{II}}_2$ unit in the absence of any exchange coupling. Upon a decrease in the temperature, $\chi_M T$ values increase slowly and reach 3.58 and 3.57 emu K mol^{-1} at 80 K for **1** and **2**, respectively, and then they abruptly increase, reaching the maximum values of 5.79 and 6.14 emu K mol^{-1} at approximately 9 K for **1** and **2**, suggesting ferromagnetic coupling between Ni$^{\mathrm{II}}$ and Fe$^{\mathrm{III}}$ ions. The maximum value at 9 K is in good agreement with an $S = 3$ ground state. After 9 K, the $\chi_M T$ values decrease to 2.93 and 3.84 emu K mol^{-1} at 1.8 K for **1** and **2**, respectively. This magnetic behavior could be attributed to the presence of significant zero-field splitting in the ground state,[28] weak intermolecular antiferromagnetic interactions, or Zeeman effects.

The magnetization was measured in fields of up to 70 kOe, at a fixed temperature of 1.8 K. The magnetization values of 4.40 and 4.32 Nβ mol^{-1} for **1** and **2**, respectively, at 7 T are apparently unsaturated (inset of Figure 5) and confirm their $S = 3$ ground state. The low-field magnetization values are fitted well with the Brillouin curve corresponding to $S = 3$ and are higher than those of the Brillouin curve for noninteracting $S = 2S_{\mathrm{Fe}}^{\mathrm{III}} + 2S_{\mathrm{Cu}}^{\mathrm{II}}$ with $g = 2.0$, further confirming the overall ferromagnetic Ni$^{\mathrm{II}}$−Fe$^{\mathrm{III}}$ interaction. The high-field magnetizations are lower than the calculated values, which may be due to the zero-field-splitting effect.

According to the structures, an approximate isotropic Hamiltonian can be described as $\hat{H} = -2J[\hat{S}_{\mathrm{Fe1}}(\hat{S}_{\mathrm{Ni1}} + \hat{S}_{\mathrm{Ni2}}) + \hat{S}_{\mathrm{Fe2}}(\hat{S}_{\mathrm{Ni1}} + \hat{S}_{\mathrm{Ni2}})]$, and the van Vleck expression can be written as[5a,15a]

$$\chi_M = \frac{2Ng^2\beta^2}{kT} \frac{7 + e^{-2J/kT} + 10e^{2J/kT} + e^{-6J/kT} + 14e^{4J/kT}}{12 + e^{-4J/kT} + 8e^{-2J/kT} + 5e^{2J/kT} + 3e^{-6J/kT} + 7e^{4J/kT}} \quad (1)$$

In order to minimize the anisotropy effects, least-squares fittings of the experimental data using eq 1 were carried out above 9 K, taking into account the intermolecular interactions (zJ') within the mean-field approximation, leading to $g = 2.14$, $J = +4.26$ cm^{-1}, and $zJ' = -0.056$ cm^{-1} with $R = 2.40 \times 10^{-3}$ for **1** and $g = 2.14$, $J = +4.18$ cm^{-1}, and $zJ' = -0.011$ cm^{-1} with $R = 2.13 \times 10^{-3}$ for **2**. The sign and relative magnitudes of the exchange parameters in **1** and **2** are comparable to those of similar clusters.[5a,15a]

In the M vs H/T plot, a nonsuperposition of the lines in different magnetic fields is observed (Figure 6), suggesting the existence of zero-field splitting in **1** and **2**. With the spin ground state $S = 3$, fits of the magnetization data using *ANISOFIT 2.0*[29] for $T \leq 5$ K and $H > 1$ T afforded

---

(28) Mydosh, J. A. *Spin glasses: An Experimental Introduction*; Taylor & Francis: London, 1993.

(29) Shores, M. P.; Sokol, J. J.; Long, J. R. *J. Am. Chem. Soc.* **2002**, *124*, 2279.

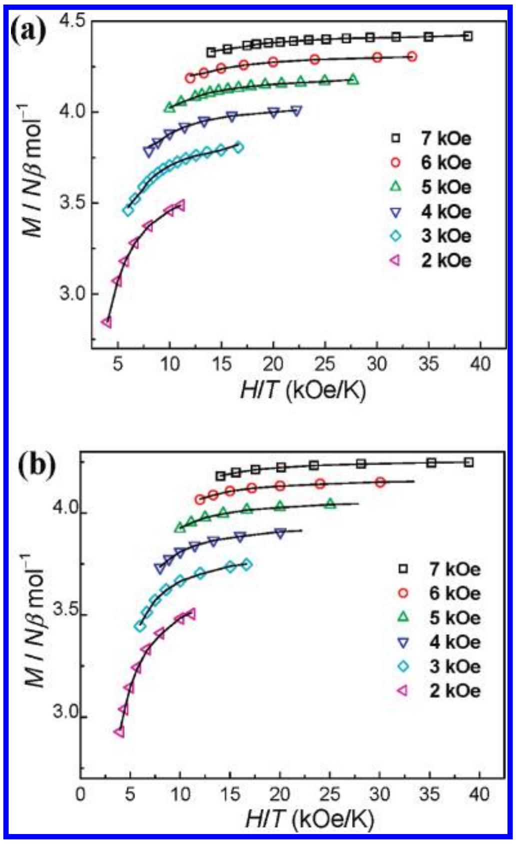

Figure 6. Plots of magnetization vs H/T for **1** (a) and **2** (b) between 1.8 and 5.0 K. The solid lines represent fits to the data.

$D = -2.85$ and -3.04 cm^{-1} and $g = 2.20$ and 2.16 for **1** and **2**, respectively. The g and D values are comparable to those of the reported cyano-bridged cluster containing Fe^{III} and Ni^{II} ions.[5a,15a]

To investigate the dynamic nature, ac magnetic measurements were performed in a 5 Oe ac field oscillating at 1−1488 Hz in the temperature range of 1.8−5 K with zero dc field (Figures 7 and 8). The obvious frequency-dependent signals in both in-phase (χ_M') and out-of-phase (χ_M'') susceptibilities can be observed. The χ_M'' values for a given frequency attain a maximum that shifts to lower temperature upon a decrease in the frequency. The χ_M'' peak positions were determined by using fits to Lorentzian lines, and the plots of ln τ vs $1/T$ follow the Arrhenius expression $\ln \tau = U_{eff}/k_BT + \ln \tau_0$, where τ, τ_0, U_{eff}, and k_B represent the relaxation time, preexponential factor, relaxation energy barrier, and Boltzmann constant, respectively. Least-squares fittings gave $\tau_0 = 4.9 \times 10^{-7}$ s for **1** and 1.1×10^{-7} s for **2** and effective spin-reversal barriers of $U_{eff} = 8.7$ K for **1** and 13.5 K for **2**. The χ_M' and χ_M'' signals indicate the existence of slow magnetization relaxation and support the fact that **1** and **2** behave like SMMs, although weak intermolecular $\pi-\pi$ interactions exist in the structures.[5a,7a]

At room temperature, the χ_MT value of complex **3** is 2.44 emu K mol^{-1} (Figure 9), which is slightly higher than the spin-only value of 1.75 emu K mol^{-1} expected for two low-spin Fe^{III} ($S = {}^1/_2$) and one Ni^{II} ($S = 1$) in the absence of any exchange coupling. In the 300−50 K temperature range, χ_MT increases in a mild way with a decrease in the temperature, followed by a rapid increase to a maximum of 3.39 emu K mol^{-1} at 9 K, which is ascribed to the ferromagnetic coupling between Fe^{III} and Ni^{II} ions. The magnetization at saturation per Fe$^{III}{}_2$Ni^{II} unit is 3.51 Nβ mol^{-1} at 7 T, suggesting $S = 2$ for **3** (inset of Figure 6), which can be confirmed by the simulation of Brillouin curves corresponding to both $S = 2$ and noninteracting $S = S_{Ni} + 2S_{Fe}$ with $g = 2.0$. Below 9 K, χ_MT drops sharply and reaches a value of 2.17 emu K mol^{-1} at 1.8 K. According to the structure, the exchange Hamiltonians of **3** can be described as follows: $\check{H} = -2J(\hat{S}_{Fe1}\hat{S}_{Ni1} + \hat{S}_{Ni1}\hat{S}_{Fe1A})$, which includes only the nearest-neighbor exchange. The van Vleck expression can be written as

$$\chi_M = \frac{2Ng^2\beta^2}{kT}\,\frac{1 + 5e^{2J/kT} + e^{-2J/kT}}{3 + 5e^{2J/kT} + 3e^{-2J/kT} + e^{-4J/kT}} \qquad (2)$$

The best fit between 10 and 300 K with eq 2 taking into account the intermolecular interactions (zJ') within the mean-field approximation gives $g = 2.34$, $J = +4.10$ cm^{-1}, and $zJ' = -0.064$ cm^{-1}, and the agreement factor (R) is 3.4×10^{-4}. The ac susceptibility studies carried out in the 1.8−10 K range in a 5 Oe oscillating field at frequencies of up to 1500 Hz for **3** showed no evidence for magnetic ordering or slow paramagnetic relaxation. Compared with complexes **1** and **2**, the results may be reasonable because much stronger intermolecular interactions are observed in **3**.

The temperature dependence of susceptibility for complex **4** appears to be dominated by spin−orbit coupling effects exhibited by the Co^{II} centers (Figure 10).[30] At

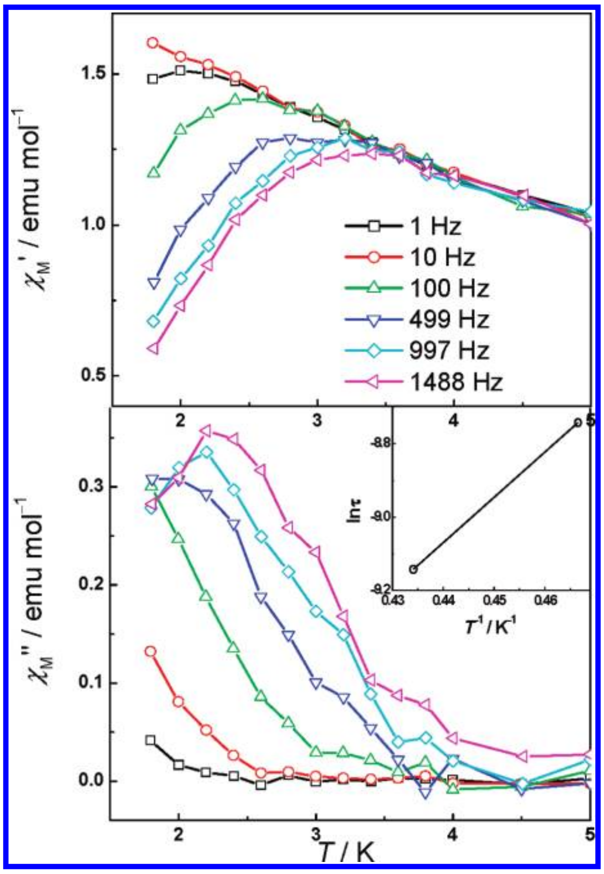

Figure 7. Frequency dependencies of the in-phase χ_M' and out-of-phase χ_M'' products vs T for **1** in a 5 Oe ac field oscillating at frequencies between 1 and 1488 Hz under a zero dc field. Inset: Arrhenius fit for the ln τ vs T^{-1} plot.

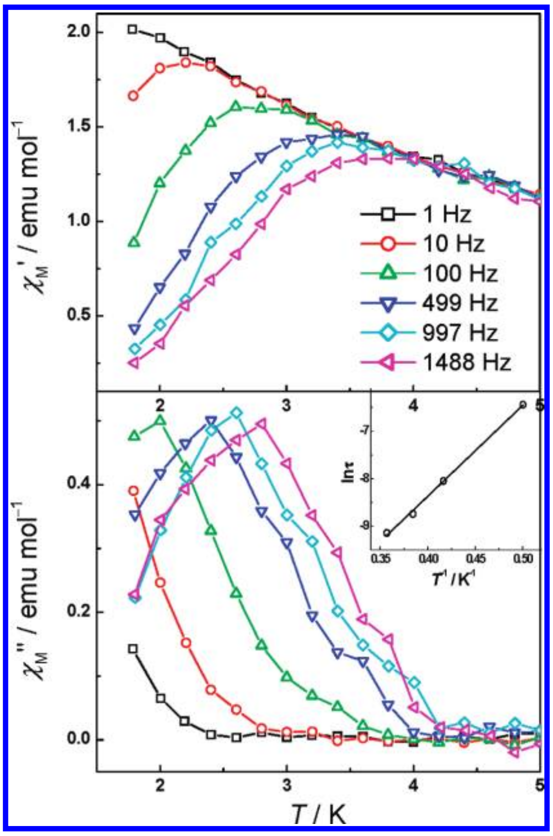

Figure 8. Frequency dependencies of the in-phase χ_M' and out-of-phase χ_M'' products vs T for **2** in a 5 Oe ac field oscillating at frequencies between 1 and 1488 Hz under a zero dc field. Inset: Arrhenius fit for the ln τ vs T^{-1} plot.

room temperature, the $\chi_M T$ value of 6.02 emu K mol^{-1} is much higher than the expected spin-only value of 2.63 emu K mol^{-1} per Fe$_2$Co unit (g_{Fe} = g_{Co} = 2, S_{Fe} = $^1/_2$, and S_{Co} = $^3/_2$). As the temperature is lowered, first $\chi_M T$ decreases, attains a minimum at T_{min} = 35 K with $\chi_M T$ = 5.44 emu K mol^{-1}, and then increases sharply to a maximum of 11.28 emu K mol^{-1} at 3.1 K. Below this temperature, $\chi_M T$ decreases abruptly and reaches a value of 6.77 emu K mol^{-1} at 1.8 K. The presence of a minimum is probably due to depopulation of thermally populated low-lying excited states for the S = $^3/_2$ Co^{II} centers or due to the magnetic anisotropy of Co^{II}.[30] The maximum of $\chi_M T$ below T_{min} indicates a ferromagnetic coupling between Fe^{III} and Co^{II} ions. We cannot find an appropriate model to represent the magnetic susceptibility and evaluate the exchange parameter between low-spin Fe^{III} and high-spin Co^{II} centers. The field-dependent magnetization with ca. M = 4.97 Nβ mol^{-1} at 7 T shows the magnetization value expected for a ferromagnetically coupled Fe$^{III}_2$Co^{II} unit. A comparison between calculations based on the Brillouin function and the observed curves is shown in the inset of Figure 7. The absence of an χ_M'' signal suggests a lack of SMM behavior above 1.8 K for **4**.

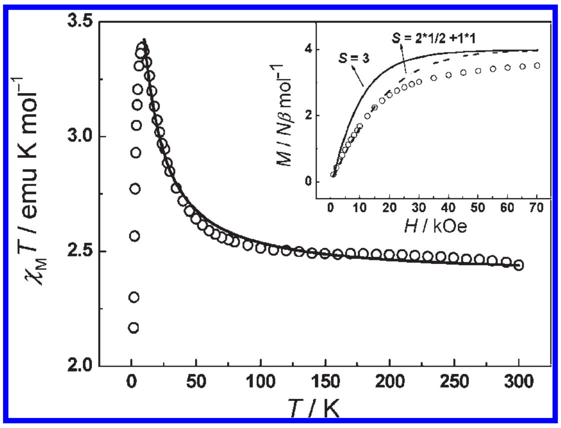

Figure 9. Temperature dependence of $\chi_M T$ in the dc field of 2 kOe for **3**. The solid line corresponds to the best-fit curve. The inset shows magnetization versus the applied magnetic field at 1.8 K; the lines represent the Brillouin function that corresponds to noninteracting $S = 2S_{Fe}{}^{III} + S_{Ni}{}^{II}$ (dotted) and S = 2 (solid) with g = 2.0.

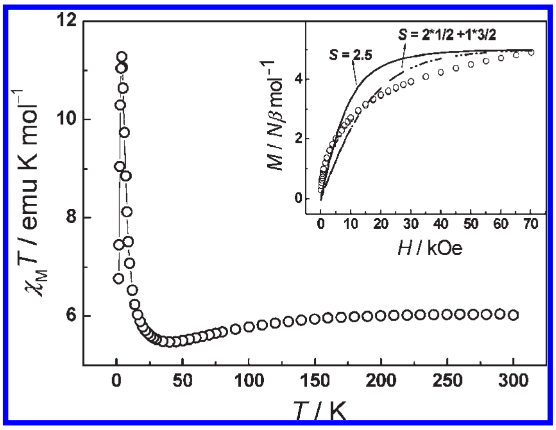

Figure 10. Temperature dependence of $\chi_M T$ in the dc field of 2 kOe for **4**. The inset shows magnetization versus the applied magnetic field at 1.8 K. The lines represent the Brillouin function that corresponds to noninteracting $S = 2S_{Fe}{}^{III} + S_{Co}{}^{II}$ (dotted) and S = 2.5 (solid) with g = 2.0.

In conclusion, with the use of π-conjugated 1,3-dithiol-2-ylidene-containing ligands and tailored tricyanometalate building blocks, two rectangular square clusters and two trinuclear clusters have been prepared. Complexes **1** and **2** show SMM behavior with effective spin-reversal barriers of 8.7 and 13.5 K, respectively. Further investigations on these types of clusters with other π-conjugated tetrathiafulvalene derivatives are currently underway in our laboratory, and our goal is to construct conductive SMMs or molecular magnetic semiconductors.

Acknowledgment. This work was supported by the Major State Basic Research Development Program (Grants 2006CB806104 and 2007CB925103), the National Science Fund for Distinguished Young Scholars of China (Grant 20725104), and the National Natural Science Foundation of China (Grant 20721002).

Supporting Information Available: X-ray crystallographic files in CIF format for **1**−**4**, selected bond distances and angles (Tables S1−S4), structures (Figures S1−S7), and additional magnetic data (Figures S8 and S9). This material is available free of charge via the Internet at http://pubs.acs.org.

---

[30] (a) Li, D. F.; Parkin, S.; Wang, G. B.; Yee, G. T.; Prosvirin, A. V.; Holmes, S. M. *Inorg. Chem.* **2005**, *44*, 4903. (b) Brechin, E. K.; Cador, O.; Caneschi, A.; Cadiou, C.; Harris, S. G.; Parsous, S.; Vonci, M.; Winpenny, R. E. P. *Chem. Commun.* **2002**, 1860. (c) Plater, M. J.; Foreman, M. R. S. J.; Coronado, E.; Gómez-García, C. G.; Slawin, A. M. Z. *J. Chem. Soc., Dalton Trans.* **1999**, 4209. (d) Gu, Z. G.; Yang, Q. F.; Liu, W.; Song, Y.; Li, Y. Z.; Zuo, J. L.; You, X. Z. *Inorg. Chem.* **2006**, *45*, 8895.